H15-114
POLLUTANT REMOVAL MECHANISM FOR IDEALIZED 2D URBAN STREET CANYONS

Chun-Ho Liu, W.C. Cheng, Tracy N.H. Chung, Colman C.C. Wong, and Pieta K.K. Leung

Department of Mechanical Engineering, The University of Hong Kong, Hong Kong

INTRODUCTION
Pollutant removal from the ground level of street canyons has long been an attractive research topic in the urban meteorology community. In view of the rapid urbanization across the globe, an in-depth understanding of the pollutant transport processes in the vicinity to urban roughness elements is necessary to safeguard the heath of urban inhabitants nowadays.

In this paper, the large-eddy simulation (LES) is employed to elucidate the pollutant removal mechanism from street canyons to the urban boundary layer (UBL) aloft. Hypothetical urban roughness elements, which are constructed by identical 2D street canyons, are used to build an idealized urban area. The building-height-to-street-width (aspect) ratio is the key geometry parameter controlling the aerodynamic roughness and flow characteristics. In this preliminary attempt, the prevailing flow is normal to the axis of street canyon of unity aspect ratio (skimming flow regime) in order to consider the worst scenario of pollutant removal.

METHODOLOGY
LES of the open-source CFD code, OpenFOAM (*OpenFOAM* 2011) is adopted. The flows are assumed to be isothermal and incompressible, consisting of the continuity and the Navier-Stokes equations. The subgrid-scale (SGS) Reynolds stresses are modelled by the Smagorinsky model (*Smagorinsky* 1963) and the one-equation SGS turbulent kinetic energy (TKE) conservation (*Schumann* 1975). The advection-diffusion equation is used to handle the pollutant conservation in which the SGS pollutant fluxes are modelled by eddy-diffusivity.

COMPUTATIONAL DOMAIN AND BOUNDARY CONDITIONS
The LES computational domain is comprised of identical 2D street canyons evenly placed in cross flows (Figure 1). It is homogeneous in the spanwise direction y that consists of 37 identical buildings of size h (height) $\times w$ (length) $\times l$ (width). These buildings are placed at b apart that constructs 36 idealized 2D street canyons of aspect ratio h/b. The building width w is equal to $10h$, while the building height and length are equal to the building separation ($h = l = b$) so the aspect ratio is unity. Over the buildings is the UBL of height H ($= 9h$).

NUMERICAL METHODS AND DISCRETIZATION
The implicit second-order accurate backward differencing is used in the temporal domain integration. The second-order accurate Gaussian finite volume integration scheme is adopted to calculate the gradient, divergence, and Laplacian terms. The values on cell faces are interpolated by the central differencing of the values at cell centres. The gradient normal to a surface (used in the Laplacian terms) is corrected by the explicit non-orthogonal method.

Stretched meshes are used in the current LES. The first element is placed at $z^+ \approx 5$ (in wall unit) away from the nearby solid boundary so the spatial resolution is fine enough to use the logarithmic velocity profile handling the near-wall flows. The LES is integrated over 2,000 h/U at a time increment 0.01 h/U to activate the turbulence to pseudo-steady state. The flow variables are then collected for a time of 200 h/U for post-processing. The Reynolds number (~12,000) based on the characteristic speed and length scales is well over the critical value.
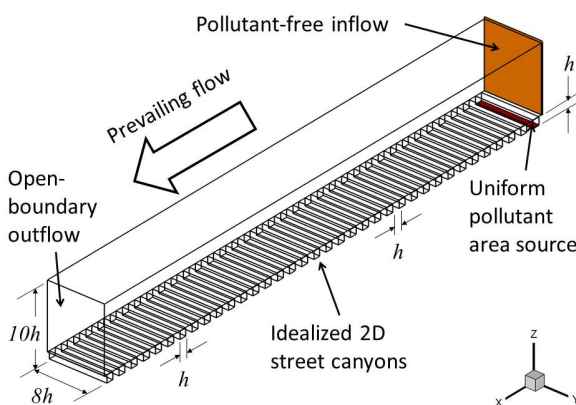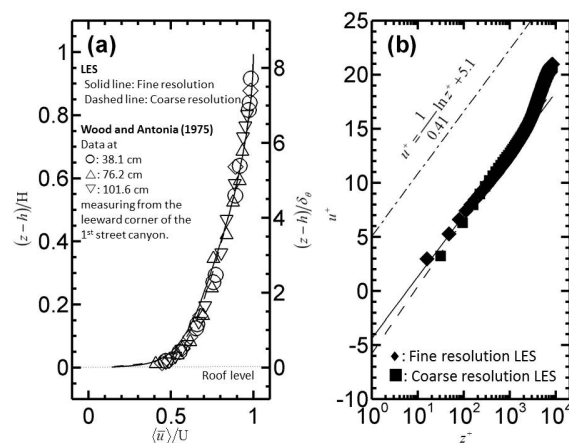

Fig. 1: Computational domain.

Fig. 2: Vertical profiles of mean streamwise velocity in (a) global and (b) wall units.

RESULTS AND DISCUSSION
Mean velocity, turbulence, and skewness
The vertical profiles (ensemble averaged in time and horizontal directions, represented by <•>) of streamwise velocity of *Wood and Antonia* (1975) and the current LES are compared well with each other (Figure 2a). They are scaled by the momentum thickness δ_θ in the global scales because of the developing turbulent boundary layer being investigated in *Wood and Antonia* (1975). The velocity gradient in the vicinity to the bottom building roughness elements is slightly higher than that of the LES mainly because of the higher Reynolds number in the experiments of *Wood and Antonia* (1975).

In classical turbulence theory, the effect of surface roughness on isothermal shear flows, analogous to its smooth-wall counterpart, is described by the logarithmic velocity profile:
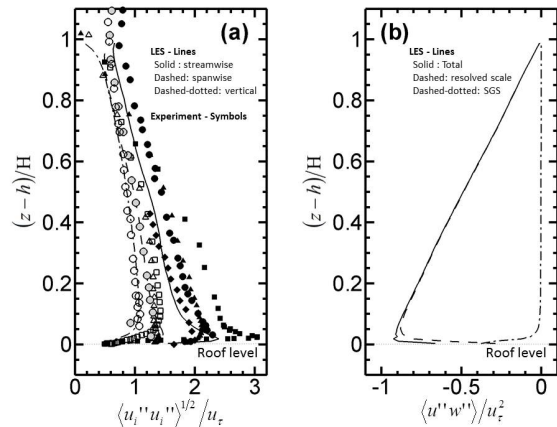

Fig. 3; Vertical profiles of (a) velocity fluctuations and (b) vertical momentum flux. Lines are the current LES. Symbols are the data from Djenidi et al. (1999) □, Krogstad and Antonia (1999) Δ, and Burattini et al. (2008) ○. Also shown are the DNS of Coceal et al. (2007) ◊. Streamwise, spanwise, and vertical components are represented by filled, shaded, and empty symbols, respectively.

Fig. 4; Vertical profiles of skewness of (a) streamwise $S_{\bar{u}}$ and (b) vertical $S_{\bar{w}}$ velocity at different locations. Lines are the LES at x/h := 0 (solid), ±0.25 (dashed), ±0.4 (dashed-dotted), and ±0.75 (dashed-dotted-dotted). Symbols are the wind tunnel measurement by Brown et al. (2000) at x/h := 0 (filled), ±0.25 (shaded), and ±0.4 (empty).

$$u^+ = \frac{1}{\kappa}\ln z^+ + A^+ - \Delta u^+ \tag{1}$$

where ε (= 0.41) is the von Karman constant, A^+ (= 5.1) an empirical constant independent from the geometry of roughness elements, and Δu^+ the roughness function (or shift in mean velocity). The roughness function accounts for the effects of surface roughness on the flows, leading to the departure of mean velocity from its smooth-wall counterpart. Superscripts + signify that the flow quantities are measured in wall units. The velocity profiles based on the current LES data exhibit a logarithmic behaviour in which the von Karman constant is found to be 0.405. Comparing with the velocity profile over a smooth wall the roughness function of the current LES for idealized 2D street canyons of unity aspect ratio equals 9.434.

Figure 3a compares the vertical profiles of velocity fluctuations over 2D urban street canyons collected from various laboratory data and the current LES. The experimental data exhibit a range of maximum streamwise velocity fluctuation ($2u_\tau < <u''u''>^{1/2} < 3u_\tau$, where u_τ is the friction velocity) which is consistently peaked close to the roof level of the buildings. The profile of spanwise velocity fluctuation is similar to its streamwise counterpart whose maximum ($<v''v''>^{1/2} = 1.3u_\tau$) locates slightly over that of the streamwise component at $z = 0.05H$ above the building roughness elements. The vertical velocity fluctuation is least among the three components whose broad maximum ($<w''w''>^{1/2} = 1.1u_\tau$) is peaked in $0.05H < z < 0.2H$. Nevertheless, the current LES results, including all the three velocity components, fall well within the sparse experimental data.

Figure 3b shows the profile of (total) vertical momentum flux $<u''w''>$ and its partitions into the resolved-scale and SGS components. As expected, the SGS vertical momentum flux is negligible except close to the building roof. On the other hand, the resolved-scale counterpart dominates the transport in the UBL core. The sum of the resolved-scale and SGS is the total vertical momentum flux that decreases linearly with increasing elevation from the buildings.

Skewness measures the asymmetry of the probability distribution of the velocity samples (Figure 4). The streamwise velocity along the street canyon roof level is positive skewed (Figure 4a) while the vertical component is quite symmetry (Figure 4b). As such, it is expected that narrow (massive) fast (slow) moving air masses are observed right over the building roughness elements. The fast (slow) moving air masses in fact govern the pollutant removal (fresh air entrainment) whose mechanism is detailed in the next section.

Coherent structures
Additional insight of the flows, transport processes, and pollutant removal mechanism can be earned from the coherent structures in the UBL over street canyons. Coherent structures are the snapshots of the flows that are taken as the typical flow behaviors.
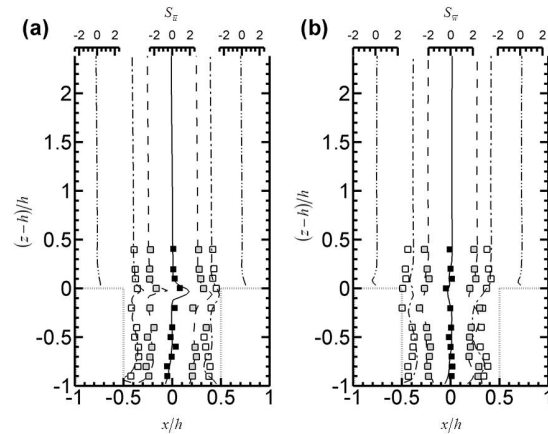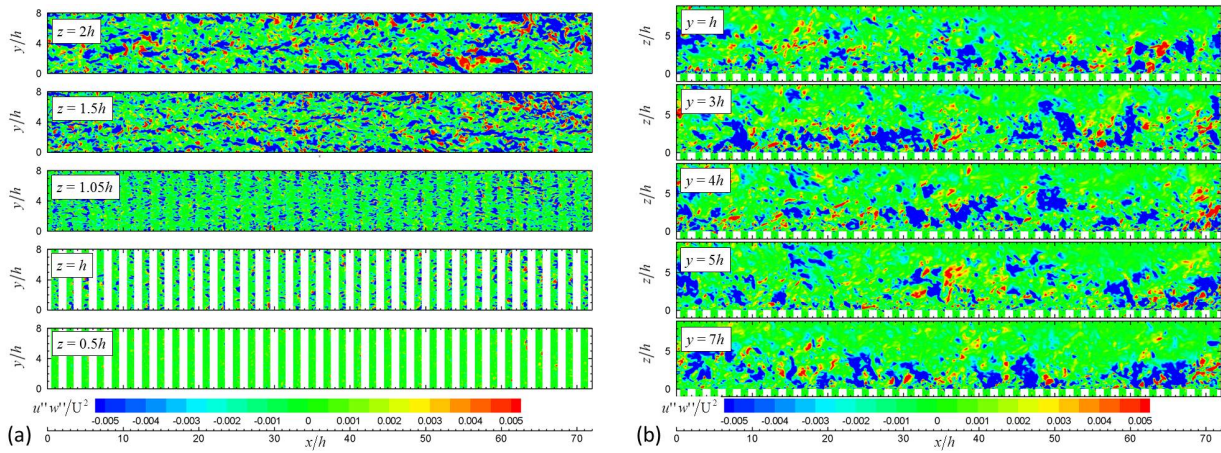
Fig. 5: Snapshot of fluctuating vertical momentum flux u''w'' on different transverses on the (a) horizontal x-y and (b) vertical x-z planes.

Figure 5a compares the vertical momentum flux on the horizontal *x-y* planes at different elevations over the buildings. Large, mildly elongated coherent structures are clearly observed in the UBL core ($z \geq 1.5h$). They break down into pieces when the flow is descending toward the building roughness elements. Because of the building roof, those air masses carrying (downward) vertical momentum flux concentrate over the roof of street canyons ($z = 1.05h$). Eventually, the descending air masses carry the momentum into the street canyons on the windward side ($z = h$). Owing to the recirculating flows in the street canyons, the downward flows dissipate quickly, leaving insignificant upward momentum flux in the mid-level of the street canyons.

Figure 5b depicts the spatial contours of vertical momentum flux on various vertical *x-z* planes. They are more packed in the lower part of the UBL because of the sharp velocity gradient right over the building roughness elements. It is noteworthy that the UBL is dominated by negative vertical momentum flux. Hence, the momentum at the street or the near-roof levels is largely attributed to the descending flows from the top of the UBL.
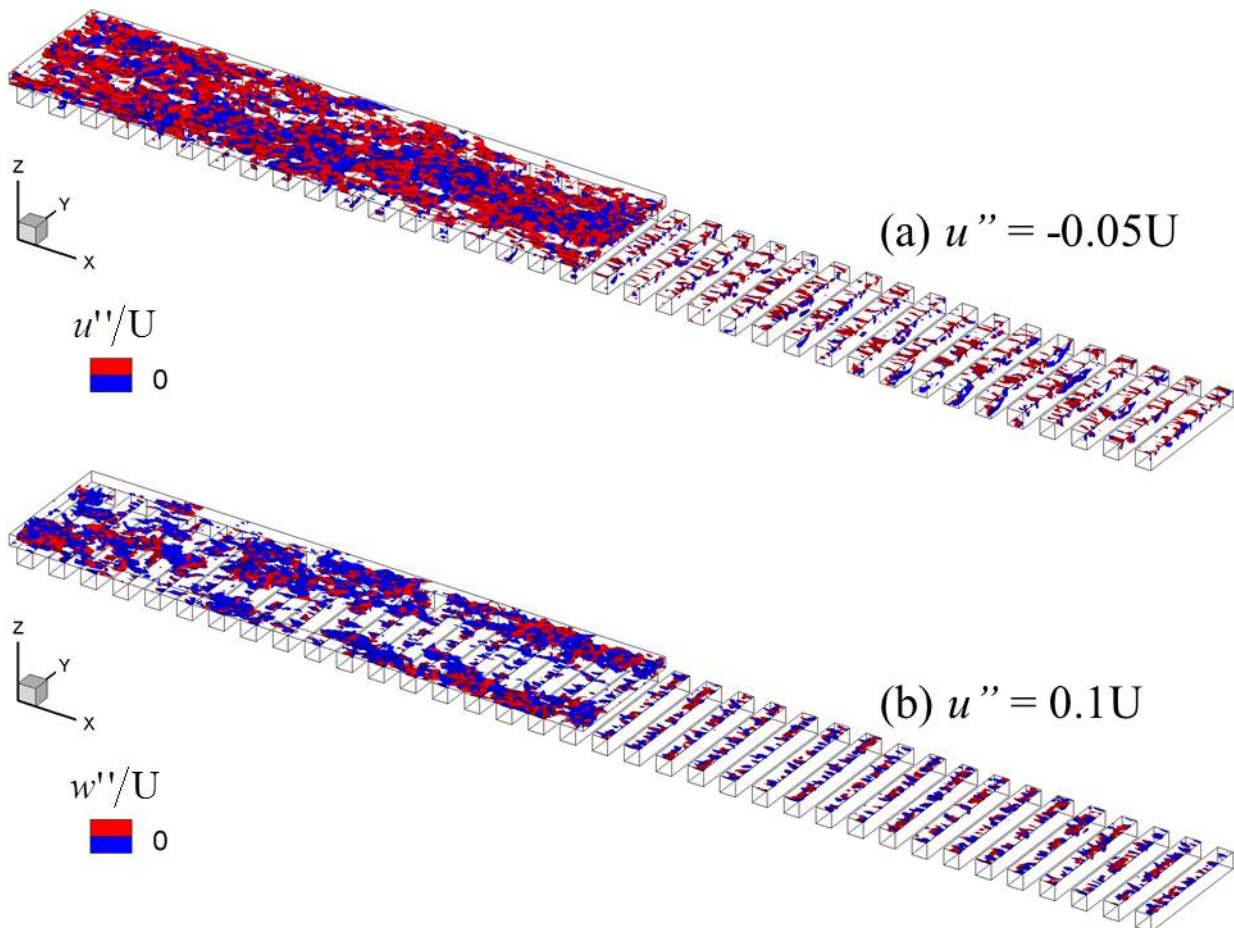

Fig. 6: Snapshot of isosurfaces of fluctuating streamwise velocity u'' = (a) -0.05U (deceleration) and (b) 0.1U (acceleration). Also shown on the isosurfaces are the contours of fluctuating vertical velocity w''.

Figure 6 illustrates the correlation between the streamwise and vertical flows in the vicinity to the building roughness elements. The decelerating air masses (Figure 6a; $u'' = -0.05U$) over the buildings are evenly distributed into upward and downward flows in the UBL over the buildings. When descends to the roof level, decelerating air masses cover the entire roof of street canyons. In view of the majority of negative vertical momentum flux, the roof-level decelerating air masses come along with upward flows. The uprising air masses in turn carry aged air and pollutants from the street canyons to the UBL aloft. This flow and transport coupling are clearly shown in Figure 6a (by the dominated red contours).

On the contrary, accelerating roof-level air masses are more packed on the windward side of the street canyons (Figure 6b; $u'' = 0.1U$). As momentum is largely provided from the upper UBL, the descending air masses drive the flows together with fresh air from the UBL into the street canyons. This entrainment purges aged air and pollutants from the street canyons.

CONCLUSION

LES is performed to elucidate the flows, transport processes, and pollutant removal mechanism over idealized urban areas. A simplified computational domain, consisting of 36 identical 2D street canyons, is used in the LES. Using a term to handle the velocity shift, the mean flows over the buildings exhibit a logarithmic layer similar to its counterpart over a smooth wall. The streamwise velocity fluctuation is peaked at the roof level, while the maxima of spanwise and vertical components are elevated over the buildings. Besides, vertical momentum decreases almost linearly with increasing height. Analysis of the skewness of turbulence data reveals that narrow, fast-moving air masses are packed along the roof level of street canyons. Moreover, accelerating (decelerating) air masses are associated with descending fresh (ascending aged) air, suggesting the basic pollutant removal mechanism for 2D urban street canyons. Apparently, increasing urban roughness could be a means of decelerating roof-level air masses that in turn purges pollutants from the street level.

REFERENCES

Brown, M.J., R.E. Lawson, D.S. Decroix and R.L. Lee, 2000: Mean flow and turbulence measurements around a 2-D array of buildings in a wind tunnel. *11th Joint AMS/AWMA Conference in Applied Air Pollution Meteorology*, Long Beach, CA.

Burattini, P., S. Leonardi, P. Orlandi and R.A. Antonia, 2008: Comparison between experiment and direct numerical simulations in a channel flow with roughness on one wall. *J. Fluid Mech.*, **600**, 403-426.

Coceal, O., T.G. Thomas, I.P. Castro and S.E. Belcher, *2006:* Mean flow and turbulence statistics over groups of urban-like cubical obstacles. *Boundary-Layer Meteorol., 121, 491-519.*

Djenidi, L., R. Elavarasan and R.A. Antonia, 1999: The turbulent boundary layer over transverse square cavities, *J. Fluid Mech.*, **395**, 271-294.

Krogstad, P.-A. and R.A. Antonia, R.A. 1999: Surface roughness effects in turbulent boundary layers. *Expt. Fluids*, **27**, 450-460.

OpenFOAM, 2011: OpenFOAM: The open source CFD toolbox. http://www.openfoam.com/.

Schumann, U. 1975: Subgrid scale model for finite difference simulations of turbulent flows in plane channels and annuli. *J. Comp. Phys.*, **18**, 376-404.

Smagorinsky, J. 1963: General circulation experiments with the primitive equations I: the basic experiment. *Month. Weath. Rev.*, **91**, 99-165.

Wood, D.H. and R.A. Antonia, 1975: Measurements in a turbulent boundary layer over a *d*-type surface roughness. *Trance. ASME, Series E, J. App. Mech.*, **42**, 591-597.